



HAL
open science

Gain measurements of THz quantum cascade lasers using THz time-domain spectroscopy

Nathan Jukam, Sukhdeep Dhillon, Zhen-Yu Zhao, Georg Duerr, Julien Armijo, Nathanael Sirmons, Sophie Hameau, Stefano Barbieri, Pascal Filloux, Carlo Sirtori, et al.

► **To cite this version:**

Nathan Jukam, Sukhdeep Dhillon, Zhen-Yu Zhao, Georg Duerr, Julien Armijo, et al.. Gain measurements of THz quantum cascade lasers using THz time-domain spectroscopy. *IEEE Journal of Selected Topics in Quantum Electronics*, 2008, 14, pp.436. hal-00270123

HAL Id: hal-00270123

<https://hal.science/hal-00270123>

Submitted on 3 Apr 2008

HAL is a multi-disciplinary open access archive for the deposit and dissemination of scientific research documents, whether they are published or not. The documents may come from teaching and research institutions in France or abroad, or from public or private research centers.

L'archive ouverte pluridisciplinaire **HAL**, est destinée au dépôt et à la diffusion de documents scientifiques de niveau recherche, publiés ou non, émanant des établissements d'enseignement et de recherche français ou étrangers, des laboratoires publics ou privés.

Gain Measurements of THz Quantum Cascade Lasers using THz Time Domain Spectroscopy

N. Jukam, S. Dhillon, Z. Y. Zhao, G. Duerr, J. Armijo, N. Sirmons, S. Hameau,

S. Barbieri, P. Filloux, C. Sirtori, X. Marcadet and J. Tignon

Abstract—Terahertz (THz) time domain spectroscopy is used to investigate the gain and losses of a THz quantum cascade laser (QCL) operating at 2.86THz. This measurement technique allows access to the amplitude and phase spectra, allowing the direct determination of the gain. At the emission frequency of the QCL, a value of 6.5cm^{-1} is found. The gain can also be studied as a function of different operating conditions, even when no laser action is present. Effects such as gain clamping and spectral narrowing are also observed. Furthermore, temperature measurements illustrate the reduction of the gain as the temperature is increased.

Index Terms—Semiconductor Lasers, quantum well devices, time domain measurements, gain measurement.

I. INTRODUCTION

TERAHERTZ (THz) quantum cascade lasers (QCL) have shown considerable development over the last few years with operation extended to low frequencies [1], sub-wavelength dimensions [2,3] and above liquid nitrogen temperature operation [4,5]. Current challenges, however, include further performance improvements and an understanding of the fundamental mechanisms within the QCL. To achieve these goals, novel characterisation methods are required to determine the key parameters such as the spectral gain and loss and dynamics that govern the QCL performance in this challenging frequency range. In this work we use THz time domain spectroscopy (TDS) [6-8] to characterise a THz QCL and show that this technique has clear advantages

Manuscript received September 1, 2007. This work was financially supported by the Délégation Générale pour l'Armement (DGA) and the Agence Nationale pour la Recherche (ANR).

N. Jukam, S. Dhillon, Z.Zhao, G. Duerr, J. Armijo, N. Sirmons, S. Hameau and J. Tignon are with the Laboratoire Pierre Aigrain, Ecole Normale Supérieure, 24 rue Lhomond, 75231 Paris Cedex 05, France (phone: +33144323507; fax: +33144323840 ; e-mail: sukhdeep.dhillon@lpa.ens.fr).

S. Barbieri, P. Filloux and C. Sirtori are with MPQ Laboratories, University Paris VII Bâtiment Condorcet, 10 rue A. Domont et L. Duquet, 75205 Paris Cedex 13, France (e-mail: stefano.barbieri@univ-paris-diderot.fr, pascal.filloux@thalesgroup.com, carlo.sirtori@univ-paris-diderot.fr).

X. Marcadet is with the III-V lab (Alcatel-Thales), Route Départementale 128, 91767 Palaiseau cedex, France (e-mail: xavier.marcadet@3-5lab.fr).

compared to more established systems that stem from the measurement of the amplitude and phase of a transmitted THz pulse. We demonstrate that it can provide useful information such as the gain and losses of a QCL and allows a feedback into new designs. Compared to previous studies [9-12] we study extensively the QCL bias and temperature dependence above and below laser threshold. In particular we show that this technique allows the probing of the gain curve over the entire operating current range.

II. THz TIME DOMAIN SPECTROSCOPY

Figure 1 shows the set-up used to characterize the QCL and is based on a standard THz-TDS system [13]. A Titanium:Sapphire (Ti:Sa) laser with 100fs pulses running at 76MHz and an average power of 0.6W is used to excite an interdigitated antenna structure to generate THz pulses. This THz source is similar to that described by Dreyhaupt *et al* [14, 15] where the interdigitated fingers are fabricated on a semi-insulating GaAs substrate. This type of structure allows a small finger separation between anode and cathode ($1.5\mu\text{m}$) and a large surface area (diameter $500\mu\text{m}$) for laser illumination. This renders redundant the use of a silicon lens to collect the THz radiation i.e. the diffraction is less compared to traditional small aperture antennas. Also the small separation of the contact fingers allows the use of relatively small voltages. Electrical pulses of only 4V with a duty cycle of 50% were applied between the two contacts. The emission was collected and focused onto the sample using a set of parabolic mirrors of F number 2. Electro-optic sampling was used to detect the THz radiation using a $200\mu\text{m}$ thick $\langle 110 \rangle$ ZnTe crystal and a probe beam from the Ti:Sa laser. The $\langle 110 \rangle$ crystal was mounted on a 2mm thick $\langle 100 \rangle$ orientated ZnTe substrate, which has a null electro-optic effect on the probe beam. This arrangement allows the elimination of any reflections of the THz radiation from the interfaces of the $200\mu\text{m}$ thick crystal. This is of importance for QCL investigations owing to the long lasting field oscillations. Finally a delay line is used on the pump beam to map out the THz electric field as a function of time. This system of

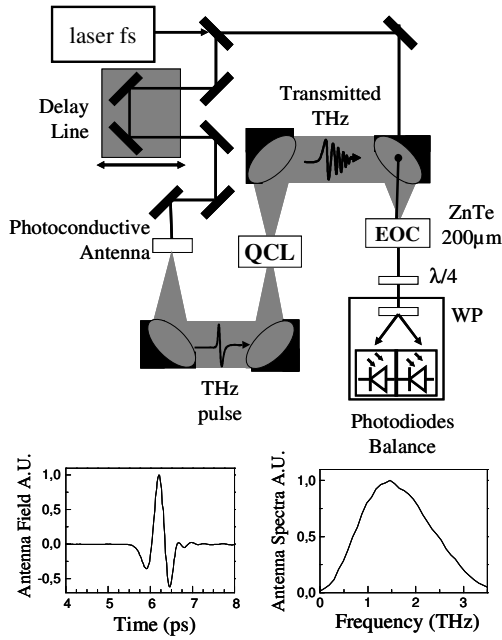


Fig. 1. Schematic of THz time domain spectroscopy set-up used to characterise the THz QCL. THz pulses are generated by a photoconductive antenna excited using a 100fs Ti:Sapph laser. These are coupled into the QCL, placed in a helium cooled cryostat. The transmitted THz pulse is detected using electro-optic sampling with a probe beam and a 200µm thick ZnTe crystal. The field and spectra from an Antenna with the QCL removed from the system are shown below the schematic.

photoconductive generation and electro-optic detection allows the realization and detection of THz pulses with electric fields over 100kV/cm with sub-picosecond pulse widths. The lower portion of Figure 1 shows a typical field scan and its spectra with the QCL removed. The useful spectral range is 0.2THz to 3.5THz with peak intensity at 1.5THz.

The device under consideration with the THz-TDS system is an AlGaAs/GaAs QCL based on a bound-to-continuum optical transition, with 90 repeats of the injector/active region unit of total thickness 12µm [4]. This device was chosen as it has been extensively characterised previously and has the advantage of low electrical power dissipation owing to the small applied electric field required for alignment. The optical confinement is based on a surface plasmon mode [16], a result of a change in sign of the dielectric constant of the metal deposited on the surface and the underlying semiconductor material (the active region in this case). Combined with the doped layer just below the active region a transverse magnetic (TM) mode as shown in figure 2 is generated. The mode, typical of this type of THz QCL, overlaps with the active region by 29% and has a significant part decaying into the substrate. Samples were processed using standard photolithography and wet chemical etching. The samples were etched to the lower doped layer, with a ridge width of 218µm and standard lateral AuGeNi contacts made. A Pd/Ge (25nm/75nm) contact, coated with a Ti/Au layer (20/100nm), was made to the top layer and centered on the laser ridge. The substrate was then thinned to approximately 200µm to aid cleaving. The inset of figure 3 shows a schematic of the

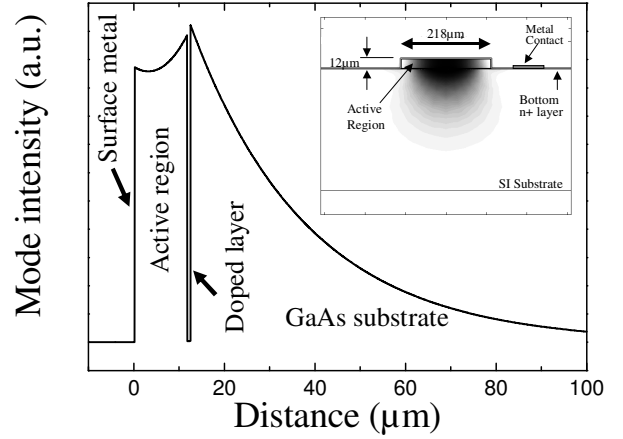


Fig 2. One dimensional transverse mode profile of the THz QCL showing typical surface plasmon confinement. (The x-axis corresponds to the growth direction with the origin taken from the surface metal). Inset shows a schematic of the realised ridge with an example of the mode profile generated

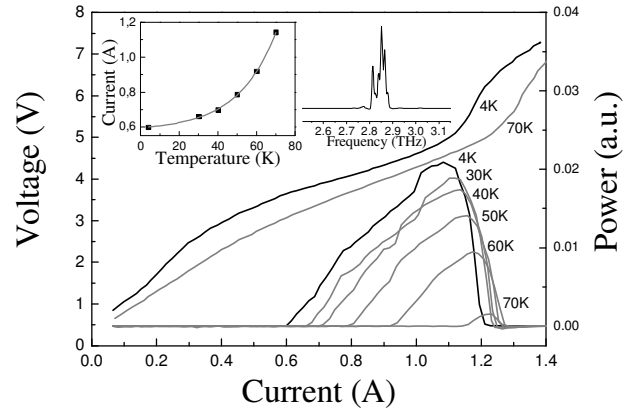


Fig 3. Pulsed electrical and optical characteristics of the THz QCL as a function of temperature. The width of the ridge is 218µm and the length of the device is 3mm. Laser action up to 70K is shown for this device. Left inset shows the threshold current as a function of temperature. Right inset shows the laser spectrum.

processed device and an example of the typical two-dimensional mode profile. Devices were cleaved into 3mm long laser bars and tested in a cold-finger cryostat equipped with the Picarin windows for in-coupling and out-coupling of the THz radiation. The temperature was measured using a thermocouple on the cold finger. The operation of the QCL was verified using a pyroelectric detector. The laser was driven at a frequency of 25kHz with a duty cycle of 25%, modulated with a 25Hz envelope to match the frequency response of the detector. The electrical and optical characteristics obtained are shown in figure 3. The voltage-current (V-I) and light current (L-I) characteristics are typical of this type of THz QCL although the conduction band misalignment observed at ~4.9V is larger than expected (2.7V) due to the large contact resistance of the top contact. At 4K a

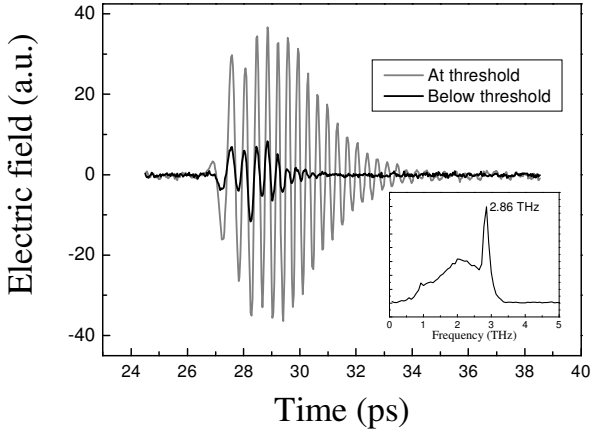


Fig 4. THz pulse coupled and transmitted through the QCL at a current (101mA) far below threshold (black line) and at the threshold current (grey line). Long lasting oscillations due to the amplification of the THz pulse at the QCL frequency are observed. The QCL is kept at a heat-sink temperature of 4.2K. Inset shows the Fourier transform of the time response showing narrow-band emission at 2.86THz.

threshold current of 0.6A ($92\text{A}/\text{cm}^2$) is observed and the maximum current before laser action stops is 1.08A ($165\text{A}/\text{cm}^2$). The maximum operating temperature of this QCL was 70K and a T_0 of 19.8K was found (see left inset of figure 2). The laser operates at a frequency of 2.86THz. The right inset shows the multi-mode (longitudinal) spectrum taken for the device at a current of 750mA showing emission around 2.86THz. The laser is single mode just above threshold.

III. AMPLIFICATION OF THZ PULSE – QCL GAIN

For the time domain measurements on the THz QCL, the antenna was modulated at 50kHz with a duty cycle of 50%. This signal was used to trigger the QCL, modulated at a frequency of 25kHz and with a 25% duty cycle. The latter was used for the lock-in reference frequency. This method allowed the detection of the transmitted THz radiation that was modulated only by the QCL and eliminated any unaffected THz radiation passing through the structure. This detection technique was necessary since the amplification of the input pulse is small at 2.9THz (The narrow bandwidth of the QCL gain overlapped only a small extremity of the antenna's bandwidth (see Fig 1).) Figure 4 shows the transmitted broadband THz pulse in time after it passes through the QCL cavity below and at laser threshold. For the former a series of oscillations are observed that die out quickly indicating a broad spectral response. At the threshold current the field shows a very different response with oscillations lasting for approximately 7ps, corresponding to an amplification of the broadband pulse at the gain of the QCL. The inset of figure 4 shows the Fourier transform of the field at threshold current. We observe a clear peak at 2.86THz i.e. at the emission frequency of the THz QCL. There is also a considerable spectral intensity at lower frequencies due to the spectral

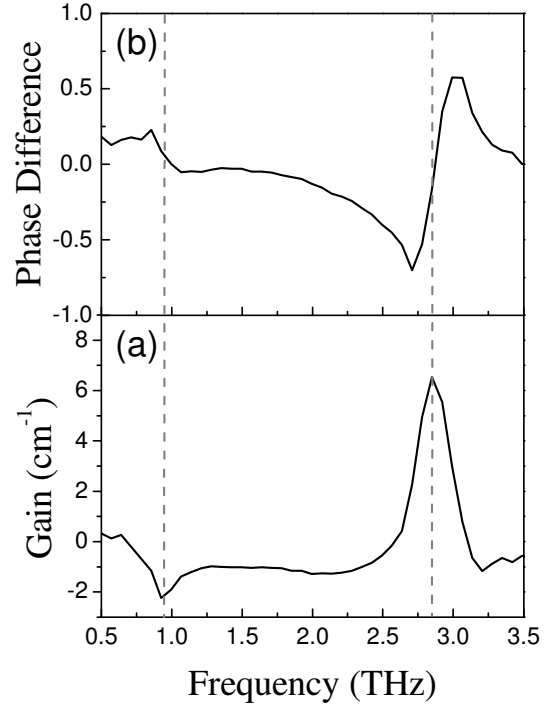


Fig 5. a) Gain spectrum of THz QCL with a driving current of 954mA. b) Corresponding phase difference spectra (in radians) showing gain at 2.86THz.

response of the antenna which falls rapidly after 1.5THz, as shown in Figure 1. This part of the spectrum is broad and corresponds to the first cycle in the time response.

From the transmitted signal, it is possible to determine the gain using a reference scan with the QCL off. An explanation of how to determine the gain and phase is presented in the Appendix. We find the curves shown in figure 5 showing the (a) gain and (b) phase spectra with a QCL current of 954mA. We find a gain of 6.5 cm^{-1} at 2.86THz. The form of the phase, with the phase being negative before the center frequency of 2.86THz (Fig. 5b), corresponds to the presence of gain. (An opposite behaviour, with the phase being positive before the center frequency and negative at higher frequencies, would be expected in the case of absorption). This is a result of the phase being equivalent to the real part of the electric susceptibility, given by $\chi'(\nu) = 2\chi''(\nu) (\nu_0 - \nu) / \Delta\nu$ (for a lorentzian resonance) where ν_0 is the center frequency and $\Delta\nu$ is the linewidth of the transition. $\chi''(\nu)$ is the imaginary susceptibility (which can be used to define the gain) and is negative for amplification and positive for absorption, resulting in the form observed in figure 5b [17].

When lasing the absorption and reflection losses from the waveguide must equal the gain. Assuming a facet reflectivity of 0.37 [18] resulting in mirror losses of 3.3cm^{-1} and a calculated free carrier absorption loss of $\alpha_g = 8\text{cm}^{-1}$, the gain of the laser is estimated to be 11.3 cm^{-1} which is significantly greater than the measured gain. The reason for this discrepancy could be the result of an underestimate of the scattering time in the Drude model, but is most likely due to

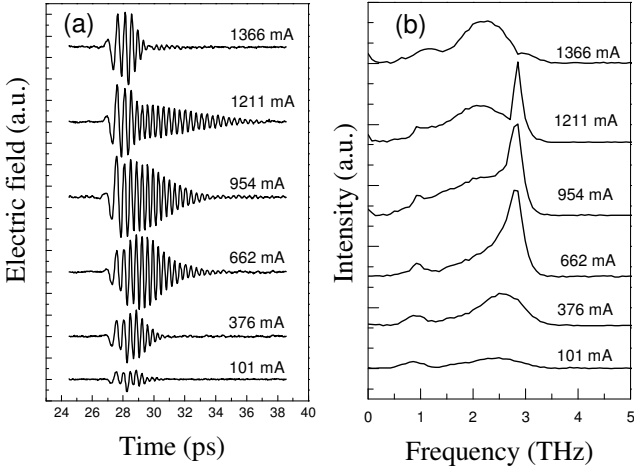


Fig 6. Measurements as a function of drive current with QCL at 10K. a) Evolution of time response of the THz QCL. b) Corresponding Fourier transformed spectra showing the change in the emission peak.

the partial coupling of the THz pulses into the higher order transverse modes of the sample [19]. The contributions from these other modes artificially increase the reference pulse and decrease the measured gain. This is due to the measurement technique (see above and Appendix). For the signal scan, the modulation frequency of the QCL is used as the reference for the lock-in amplifier and will therefore only contain the modulation (i.e. amplification) caused by the laser action of the QCL i.e. from the fundamental transverse mode shown in figure 2. However, high order transverse modes exist between the metal and substrate (in contrast to longitudinal modes that exist between the mirror facets of the device) that do not lase. Hence as the reference scan is taken with the QCL off, and the formers' modulation frequency used for the lock-in amplifier, it will contain contributions from these higher order modes. Therefore if the THz input pulse is coupled into the high order transverse modes (which have a small overlap with the active region), this will increase the reference scan and not the signal, leading to an underestimation of the gain.

The small dip in figure 5a at 0.93THz (3.8mV) is possibly to do absorption from levels within the cascade miniband. In the phase spectrum, there appears to be an inversion of the phase at this point compared to the peak at 2.86THz that is consistent with absorption. This illustrates that the THz-TDS technique allows the simultaneous measurement of both the gain/loss and the phase information of a resonance. This is in contrast to other techniques such as FT-IR spectroscopy where only the intensity is recorded.

IV. CURRENT MEASUREMENTS

The evolution of the field as a function of the QCL driving current was investigated at 10K. Figure 6a shows the fields for

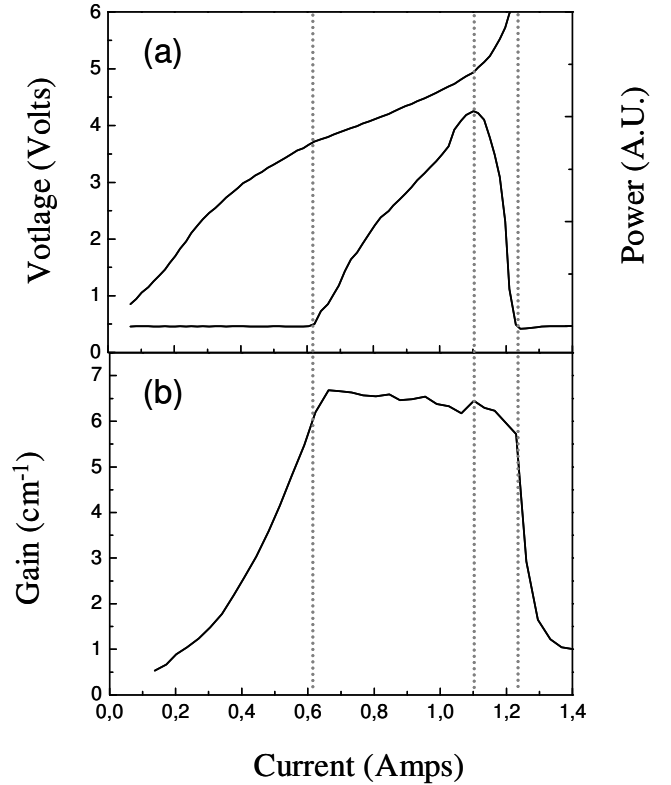


Fig 7. a) V-I and L-I of THz QCL at 10K. b) Measured gain of QCL as a function of the applied current showing gain clamping at around laser threshold. The THz QCL was kept at a heat sink temperature of 10K. The first dotted line shows the position of laser current threshold, the second the current corresponding to maximum power output of the QCL and the third where laser action has completely ceased.

currents from 101mA to 1366mA i.e. from well below threshold to beyond the maximum operating current when laser action stops. Oscillations corresponding to emission at 2.86 THz are observed as early as 200mA, considerably below threshold. The oscillations become more intense and persist longer in time as the current is increased. The corresponding spectra are shown in figure 6b and we clearly observe an increase in emission at the frequency of the QCL and a narrowing of the spectra as threshold is approached due to the alignment of the bandstructure. At 1366mA, the emission at 2.86 THz disappears due to the misalignment of the cascade structure and hence an end to laser action. As mentioned previously the feature at 0.93THz is possibly due to an absorption resonance within the QCL bandstructure. An interesting point of this THz-TDS technique is that we can examine the gain spectra of the QCL above threshold. Studies of electroluminescence spectra above threshold [20] are problematic as the signal is easily swamped by the laser emission. However, the THz-TDS measurement of the probe pulse does not detect the QCL laser emission. The phase of the QCL laser is not locked in time with the femtosecond laser pulses which measure the THz probe pulses. The femtosecond laser pulse's position in time relative to the QCL laser field will vary randomly time, and the detected signal from the QCL

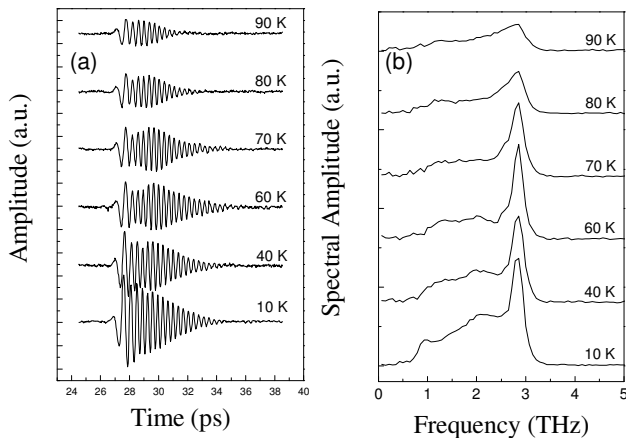


Fig 8. Measurements as a function of temperature with QCL a constant applied voltage of 4.83V. a) Time response of the THz QCL. b) Corresponding Fourier transformed spectra showing amplified emission up to 90K

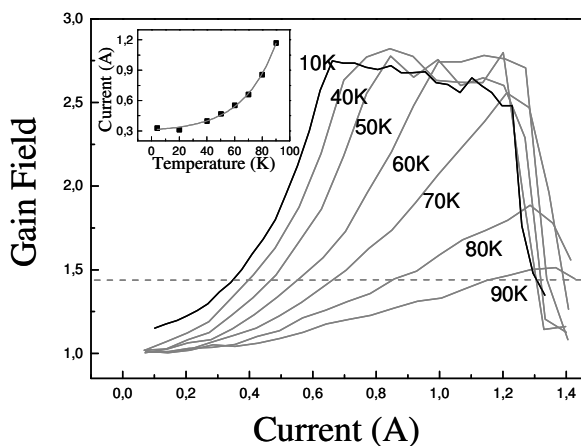


Fig 9. Gain field of the amplified emission at 2.86THz as a function of driving current for temperatures from 10K to 90K. Inset shows the evolution of the current as a function of temperature for a fixed gain (dashed grey line).

laser field will average to zero.

In figure 7 the gain is plotted as a function of injected current. Also shown for comparison are the VI and PI characteristics at 10K (Fig. 7a). Firstly the peak gain (Fig 7b) increases with increasing current due to the presence of gain even if the losses prevent laser action. The peak gain, however, saturates at 662mA (i.e. just above laser threshold at 623mA), where the gain becomes ‘clamped’ at the value of the total optical losses. (This is due to the strong negative feedback of the laser intensity on the population inversion that results in gain saturation and stabilizes the carrier density at the threshold value) [17] This behaviour is typical of lasers and semiconductor optical amplifiers (SOA) [21-23] and reported previously for a quantum cascade laser [10]. Furthermore, the gain appears to persist even after the laser action has ceased. At 1.21A, there is no further emission from the QCL. However, the input pulse continues to be amplified and it is

only at 1.3A that no further amplification is seen. This is due to the fact that gain is still present although it has become smaller than the total optical losses, inhibiting laser emission.

V. TEMPERATURE MEASUREMENTS

The temperature dependence of the transmitted pulse was also investigated. Figure 8a shows the evolution of the electric field as a function of temperature, with the QCL biased at a constant voltage of 4.83V. Oscillations corresponding to emission at 2.86THz are observed up to 90K, although the amplitude decreases rapidly after 70K. The first field cycle, corresponding to broad spectral emission, also decreases with increasing temperature. These results are also observed in the spectral domain (Fig 8b) where the intensity at 2.86THz decreases at high temperatures a result of gain reduction owing to leakage of the electrons into higher subbands and thermally activated LO phonon emission [24]. An interesting point is that gain is observed at 90K even though the laser action ceases at 70K. This hints that the temperature operation of the QCL can be extended with a reduction in the mirror and/or the waveguide losses.

The temperature measurements above are summarised in figure 9 where the gain field is plotted against the driving current for temperatures from 10K to 90K. (The gain field is defined as the ratio of the transmitted electric field with the QCL on to that with the QCL off). As previously shown in figure 6, we again observe a large increase in gain with increasing current to just below threshold where it is clamped and which slowly drops off before the structure misaligns. As the temperature is increased, the gain rises slower, reaching the clamping point at higher currents. The position of the clamping current is slightly higher than the threshold current. Using this data we can plot the change in current at a fixed gain as a function of temperature. This is shown in the inset figure 9 for a gain highlighted by the grey dotted line showing a typical exponential rise with a T_0 of 23.9K, similar to that found considering the threshold current (Fig. 3).

VI. CONCLUSION

To conclude, we have demonstrated the use of THz-TDS to investigate the gain of a QCL, showing the evolution of the gain as a function of current and demonstrating the effect of gain clamping. Furthermore, we obtain phase information directly from the measurement without resorting to the Kramers-Kronigs relations. The effect of temperature was also investigated highlighting the reduction in gain at high temperatures where the laser does not operate. Further developments will focus on QCLs operating at lower frequencies where the spectral intensity of the antenna is greater.

APPENDIX

We can write the output field at frequency ω from the QCL with the QCL on (biased) as

$$QCL(\omega) = t_{in} t_{out} \exp[-\alpha L/2 + i\Delta k_{\alpha} L] \exp[-\gamma L/2 + i\Delta k_{\gamma} L] E_{input}(\omega) \quad (A1)$$

Here t_{in} , t_{out} are the input and output coupling constants. L is the length of the waveguide. α and $\Delta k_{\alpha} L$ are the loss and the loss induced phase of the waveguide (i.e. Drude losses from the doping). γ and $\Delta k_{\gamma} L$ are the gain and gain induced phase from the QCL structure. Similarly when the QCL is turned off (not biased) the output field $R(\omega)$ can be written as

$$R(\omega) = t_{in} t_{out} \exp[-\alpha L/2 + i\Delta k_{\alpha} L] E_{input}(\omega) \quad (A2)$$

We wish to divide (A1) by (A2) to express the gain in terms of $R(\omega)$ and $QCL(\omega)$. The most obvious method is to measure the spectra with the QCL on to obtain (A1) and the QCL off to obtain (A2). However the frequency of the QCL is far away from the antenna's maximum spectral signal (shown in Figure 1), and the narrow bandwidth of the QCL gain overlaps a small portion of the antenna's broad bandwidth. The change in signal due to the QCL will be thus be small, and be on top of a large background signal. (In the time-domain $QCL(t) \sim R(t)$).

Instead we measure the difference between equations (A1) and (A2). To do this the QCL electrical pulses (which were locked in time and had the same duration as the antenna electrical pulses) were turned off for every other antenna pulse. The lock-in amplifier measured the amplitude (which we denote as $S(t)$) of the signal at the frequency at which the QCL pulses were turned on and off. (The QCL reference frequency is one half the antenna reference frequency). At the QCL reference frequency the amplitude is the difference between the signal with the QCL turned on and the signal with the QCL turned off. Thus the measured signal $S(t)$ can be written in the time-domain and frequency domains as

$$S(t) = \pm[R(t) - QCL(t)] \text{ and } S(\omega) = \pm[QCL(\omega) - R(\omega)] \quad (A3)$$

We do not know a priori whether the measured amplitude $S(t)$ corresponds to the difference $R(t) - QCL(t)$, or $QCL(t) - R(t)$. In order to resolve this ambiguity we must calculate the gain using both results and discard the results which are found to be unphysical. We can now reconstruct $QCL(t)$ from the signal $S(t)$, and the reference scan with the QCL off (i.e. $R(t)$). The complex gain can then be written as

$$\exp[-\gamma L/2 + i\Delta k_{\gamma} L] = QCL(\omega) / R(\omega) = [R(\omega) \pm S(\omega)] / [R(\omega)] \quad (A4)$$

The real component of the gain γ can be found by taking the magnitude of (A4).

$$\gamma = \frac{2}{L} \ln \left(\frac{|QCL(\omega)|}{|R(\omega)|} \right) \quad (A5)$$

The phase change $\Delta k_{\gamma} L$ caused by the gain can similarly be found by finding the phase of (A4).

$$\Delta\varphi = \Delta k_{\gamma} L = \theta_{S(\omega)} - \theta_{R(\omega)} = \arctan \left(\frac{\text{Im}[S(\omega)]\text{Re}[R(\omega)] - \text{Re}[S(\omega)]\text{Im}[R(\omega)]}{\text{Re}[S(\omega)]\text{Re}[R(\omega)] + \text{Im}[S(\omega)]\text{Im}[R(\omega)]} \right) \quad (A6)$$

where $\theta_{S(\omega)}$ and $\theta_{R(\omega)}$ are the phase of $S(\omega)$ and $R(\omega)$.

ACKNOWLEDGMENT

The Laboratoire Pierre Aigrain of the ENS is a "Unité Mixte de Recherche Associée au CNRS et aux Universités Paris 6 et 7"

REFERENCES

- [1] C. Walther, G. Scalari, J. Faist, H. Beere, and D. Ritchie, "Low frequency terahertz quantum cascade laser operating from 1.6 to 1.8 THz", *Appl. Phys. Lett.* **89**, 231121 (2006).
- [2] S. S. Dhillon, J. Alton, S. Barbieri, C. Sirtori, A. de Rossi, M. Calligaro, H. E. Beere, D. A. Ritchie, "Ultra-low threshold current THz quantum cascade lasers based on buried-strip waveguides", *Appl. Phys. Lett.*, **87**, 071107 (2005).
- [3] Y. Chassagneux, J. Palomo, R. Colombelli, S. Dhillon, C. Sirtori, H. Beere, J. Alton, D. Ritchie, "THz microcavity lasers with sub-wavelength mode volumes and thresholds in the milli-Ampere range" *Appl. Phys. Lett.* **90**, 091113 (2007).
- [4] S. Barbieri, J. Alton, H. Beere, J. Fowler, E. Linfield, and D. A. Ritchie, "2.9 THz quantum cascade lasers operating up to 70 K in continuous wave", *Appl. Phys. Lett.* **85**, 1674, (2004).
- [5] B. S. Williams, S. Kumar, Q. Hu, and J. L. Reno, "Operation of terahertz quantum-cascade lasers at 164 K in pulsed mode and at 117 K in continuous-wave mode", *Opt. Express* **13**, 3331 (2005).
- [6] D. H. Auston, K. P. Cheung, J. A. Valdmanis and D. A. Kleinman, "Cherenkov radiation from femtosecond optical pulses in electro-optic media", *Phys. Rev. Lett.* **53**, 1555 (1984).
- [7] Q. Wu and X.-C. Zhang, "Ultrafast electro-optic sensors", *Appl. Phys. Lett.* **68**, 1604 (1996).
- [8] Q. Wu, T. D. Hewitt, and X.-C. Zhang, "Two-dimensional electro-optic imaging of THz beams," *Appl. Phys. Lett.* **69**, 1026, (1996).
- [9] J. Kröll, J. Darmo, S. S. Dhillon, X. Marcadet, M. Calligaro, C. Sirtori and K. Unterrainer, "Phase resolved measurements of stimulated emission", *Nature*, Accepted for publication.
- [10] J. Kröll, J. Darmo, K. Unterrainer, S. S. Dhillon, C. Sirtori, X. Marcadet, and M. Calligaro, "Longitudinal spatial hole burning in terahertz quantum cascade lasers", *Appl. Phys. Lett.* Accepted for publication.
- [11] F. Eikenmeyer, R. A. Kaindl, M. Woerner, T. Elsaesser, S. Barbieri, P. Kruck, C. Sirtori and J. Nagle, "Large electrically induced transmission changes of GaAs/AlGaAs quantum-cascade structures", *Appl. Phys. Lett.* **76**, 3254 (2000).
- [12] F. Eikenmeyer, K. Reimann, M. Woerner, T. Elsaesser, S. Barbieri, C. Sirtori, "Ultrafast Coherent Electron Transport in Semiconductor Quantum Cascade Structures", *Phys. Rev. Lett.* **89**, 047402 (2002).
- [13] G. Zhao, R. N. Schouten, N. van der Valk, W. Th. Wenckebach and P. C. M. Planken, "Design and performance of a THz emission and detection setup based on a semi-insulating GaAs emitter", *Rev. Sci. Instrum.* **73**, 1715 (2002).

- [14] A. Dreyhaupt, S. Winnerl, T. Dekorsy, and M. Helm, "High-intensity terahertz radiation from a microstructured large-area photoconductor", *Appl. Phys. Lett.* **86**, 121114 (2005).
- [15] A. Dreyhaupt, S. Winnerl, M. Helm and T. Dekorsy, "Optimum excitation conditions for the generation of high-electric-field terahertz radiation from an oscillator-driven photoconductive device", *Opt. Lett.* **31**, 1546 (2006).
- [16] R. Köhler, A. Tredicucci, F. Beltram, H. Beere, E. H. Linfield, A. G. Davies, D. A. Ritchie, R. C. Iotti, and F. Rossi, *Nature* **417**, 156 (2002).
- [17] A. Yariv, "Optical Electronics in Modern Communications", 5th Edition, Oxford University Press, Inc, New York (1997).
- [18] J. Alton, S. S. Dhillon, A. de Rossi, M. Calligaro, H. E. Beere, S. Barbieri, E. H. Linfield, D. A. Ritchie and C. Sirtori, "Buried waveguides in THz quantum cascade lasers based on two-dimensional surface plasmon modes", *Appl. Phys. Lett.* **86**, 071109 (2005).
- [19] C. Worrall, J. Alton, M. Houghton, S. Barbieri, H. E. Beere, D. Ritchie and C. Sirtori, "Continuous wave operation of a superlattice quantum cascade laser at 2THz", *Opt. Express*. **14**, 171 (2006).
- [20] R. Colombelli, F. Capasso, C. Gmachl, A. Tredicucci, A.M. Sergent, A.L. Hutchinson, D.L. Sivco, and A.Y. Cho "Intersubband electroluminescence from long-sided-cleaved quantum-cascade lasers above threshold: Investigation of phonon bottleneck effects" *Appl. Phys. Lett.* **77**, 3893 (2000).
- [21] A. J. Bennett, R. D. Clayton, and J. M. Xu, "Above-threshold longitudinal profiling of carrier nonpinning and spatial modulation in asymmetric cavity lasers", *J. Appl. Phys.* **83**, 3784 (1998).
- [22] F. Rinner, J. Rogg, P. Friedmann, M. Mikulla, G. Weimann, and R. Poprawe, "Longitudinal carrier density measurement of high power broad area laser diodes" *Appl. Phys. Lett.* **80**, 19 (2002).
- [23] M. -S. Nomura, F. Salleras, M. A. Dupertuis, L. Kappei, D. Marti, B. Deveaud, J.-Y. Emery, A. Crottini, B. Dagens, T. Shimura and K. Kuroda, "Density clamping and longitudinal spatial hole burning in a gain-clamped semiconductor optical amplifier", *Appl. Phys. Lett.* **81**, 2692 (2002).
- [24] M. Rochat, J. Faist, M. Beck and U. Oesterle, "Electrically pumped Terahertz quantum well sources", *Physica E* **7**, 44 (2000).

Nathan Jukam received the Ph.D. degree from the University of California, Santa Barbara, in 2006. He studied terahertz photonic crystals fabricated from silicon and gallium arsenide. He is currently a Postdoctoral Fellow at the Ecole Normale Supérieure, Paris, France. His current research interests include ultra-fast spectroscopy, and quantum cascade lasers structures.

Sukhdeep Dhillon received the Ph.D. degree in 2001 from the University of Cambridge, Cambridge, U.K.

At the University of Cambridge, he was engaged in the field of far-infrared luminescence from quantum cascade structures. He is currently with the Ecole Normale Supérieure, Paris, France, as a part of the Centre National de la Recherche Scientifique. He was a Postdoctoral Fellow at Thales Research and Technology and University Paris VII, where he studied novel confinement and nonlinear optics in THz quantum cascade lasers. His current research interests include ultrafast spectroscopy of quantum well structures and magnetospectroscopy.

Zhen-Yu Zhao born in 1980. He received the B.Sc and M.Sc degrees in physics from the East China Normal University, Shanghai, China. He is currently working

toward the Ph.D. degree, as part of a France-China joint program with the University of Paris 6, Paris, France, the Ecole Normale Supérieure, Paris, and the East China Normal University, Shanghai.

Currently, in France, he is with the Group of Jerome Tignon, working on THz time domain spectroscopy and quantum cascade lasers, and in China, he is with

the Group of Zhen-Rong Sun, working on the optical properties of semiconductor nanocrystals doped niobic tellurite glasses.

Georg Duerr is with the Laboratoire Pierre Aigrain, Ecole Normale Supérieure, Paris, France, where he spent one year. He is currently a Physics Student at the Technische Universität (TUM), Munich, Germany. His current research interests include semiconductor physics and magnetism.

J. Armijo, photograph and biography not available at the time of publication.

N. Sirmons, photograph and biography not available at the time of publication.

Sophie Hameau born in 1973. She received the Ph.D. degree in 2000 from the

Ecole Normale Supérieure, Paris, France, where she studied 0D and 1D electron

systems by means for far-infrared magnetospectroscopy.

In 2001, she was a Assistant Professor at the University Paris 6, Paris, France, and joined the Y. Guldner Group at Ecole Normale Supérieure, Paris, France, where she investigated in particular polarons in quantum dots. In 2005, she joined the J. Tignon ultrafast THz Group at Ecole Normale Supérieure, Paris, and investigates QCLs and 2DEG systems.

S. Barbieri, photograph and biography not available at the time of publication.

Pascal Filloux was born in 1973. He received the Ph.D. degree in physics from

the University of Paris XI (study and fabrication of 2D photonic crystals in silicon for the near-IR), Orsay, France.

In 2004, he joined the University of Paris VII, Paris, France, as a Research Engineer. His current research interests include semiconductor device fabrication

with silicon and III-V compounds. He is a specialist in various processing techniques and has worked in several cleanroom facilities, both industrial and academic.

C. Sirtori, photograph and biography not available at the time of publication.

X. Marcadet, photograph and biography not available at the time of publication.

Jérôme Tignon born in 1969. He received the Ph.D. degree in 1996 from the Ecole Normale Supérieure, Paris, France, where he investigated the optical properties of semiconductor nanostructures.

In 1997, he joined the Lawrence Berkeley National Laboratory, Berkeley, and engaged for 2 years in the D.S. Chemla's Group, conducting research on ultrafast

phase spectroscopy of III-V semiconductors. He is currently at Ecole Normale Supérieure, Paris. He is also a Professor at the University Paris 6, Paris. His current research interests include optical nonlinear properties of semiconductor microcavities and THz ultrafast spectroscopy of semiconductor nanostructures.